

Sodium-intercalated bulk graphdiyne as an anode material for rechargeable batteries

Amir Farokh Niaei¹, Tanveer Hussain¹, Marlies Hankel¹ and Debra J. Searles^{1,2,*}

¹ *Centre for Theoretical and Computational Molecular Science, Australian Institute for Bioengineering and Nanotechnology, The University of Queensland, Brisbane, QLD 4072, Australia*

² *School of Chemistry and Molecular Biosciences, The University of Queensland, Brisbane, QLD 4072, Australia*

*Corresponding Author

Debra J. Searles

Australian Institute for Bioengineering and Nanotechnology

The University of Queensland

Brisbane, QLD 4072, Australia

Telephone: +61 7 33463939

Fax: +61 7 3346 3992

Email: d.bernhardt@uq.edu.au

Abstract

We present the results of a density functional theory study of sodium storage and mobility on graphdiyne (GDY) and consider the applicability of GDY intercalated with sodium (Na) as an anode material for rechargeable batteries. The maximum capacity, energy barriers for Na diffusion throughout the layers, and expansion of the layers due to Na insertion are determined. The calculations indicate that Na intercalates within the GDY bulk layers with a capacity of $\text{NaC}_{5.14}$ without expansion (316 mA h g^{-1}) and $\text{NaC}_{2.57}$ with expansion of 28% (497 mA h g^{-1}). The energy barrier for movement of Na in the slit pore formed by two GDY bulk layers is found to be 0.82 eV for bulk GDY with an AB-2 stacking, and the barrier for movement through a GDY sheet is found to be 0.12 eV. The barrier for movement in the slit pore formed by sheets becomes even lower for AB-3 stacking, with values of 0.68 and 0.40 eV found for different pathways. Movement from one GDY sheet to another for the AB-3 stacking also has a moderate energy of 0.37 eV. Therefore, GDY intercalated with Na is proposed to have potential as an anode material for rechargeable batteries.

Keywords: anode material; rechargeable batteries; graphdiyne; density functional theory; transition state barrier; diffusion

1. Introduction

Rechargeable batteries are widely used in many different applications as important devices for storage of energy. The ability to manufacture small, light-weight rechargeable batteries has had significant impact, with mobile phones, implantable devices and portable tools being well developed technologies that rely on rechargeable batteries. By charging the batteries using renewal energy sources, rechargeable batteries provide a way of enabling a continual supply of clean energy. However, two main problems with currently available portable batteries are their discharge time and the battery lifetime. To improve their performance, various new materials have been proposed for the anode, cathode and electrolyte. Currently the most common commercial-scale rechargeable battery is the lithium ion battery (LIB) in which lithium intercalated graphite forms the anode [1-3]. However recently, interest in sodium ion batteries (NIB) has intensified. This has been largely due to the possibility that we might exhaust the supplies of lithium due to the increasing demand for LIBs [4], and companies have already been established to advance NIB technology and make it available [5, 6]. Therefore materials for NIBs are being sought with an aim to produce a battery with high performance, with materials that are readily available at low cost.

A challenge for the replacement of Li with Na is that the Na is significantly larger than Li, with the atomic radii of Na being 1.70 Å, and 11.8% higher than Li at 1.52 Å [7]. Graphite has a very low capacity for Na because its interlayer distance of ~ 3.35 Å [8] prohibits intercalation and movement of Na within the pores created by the graphene layers [9]. The barrier for diffusion of Li through a graphene sheet is already significant, and it is higher for Na. Therefore, two-dimensional (2D) materials with a larger interlayer space and/or larger pores in the 2D sheets themselves, are required for intercalation and diffusion of Na throughout the electrode material.

Consequently, many new NIB electrode materials have been proposed both experimentally and theoretically [10-13]. Many of these are based on carbon materials due to the variety of structures that can be formed, their success in LIBs, their light weight and their conductivities. As a guide to the structure of a desirable material, Cao et al. [9] indicated that the minimum inter-layer distance for ready insertion of Na between graphitic layers should be 3.70 Å. They found that at this separation there is a moderate energy barrier for insertion of Na of 0.053 eV, which is significantly lower than the barrier of 0.12 eV when the separation is equal to that observed in graphite (note that $k_B T$ is 0.0256 eV at 298 K). Therefore, work has been carried out to develop materials with sufficient spacing between layers. An alternative approach is to use 2D sheets that have pores in them. Among these, the carbon allotrope graphdiyne (GDY) is of particular interest. GDY has 4-atom chains of carbon atoms with sp hybridization, linking 6-carbon rings with sp^2 hybridization and resulting in a 2D material with a large 18-atom triangular pore (area ~ 36 Å²), as shown in figure 1. The area of this pore is ~ 5.5 times larger than that of the 6-member rings in both graphene and GDY (~ 6.5 Å²), which suggests that Na atoms would be likely to be able to sit between the layers of GDY, even though the spacing between layers is not very much different to that in graphite.

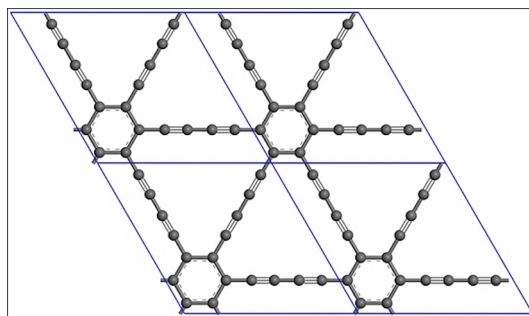


Figure 1: A schematic diagram of the 4 unit cells of GDY. Grey balls represent carbon atoms. The unit cells are marked by blue lines.

The stacking of GDY has been considered computationally by Luo et al. [14] and Zheng et al. [15]. Luo et al. identified four stacking configurations for bulk GDY with binding energies only differing by ~ 0.01 eV atom⁻¹. They found that the two AB stackings shown in figure 2, which they refer to as AB-2 and AB-3, are most stable (AB-3 slightly more stable than AB-2), and are convertible with barriers of 1.1 meV atom⁻¹ (AB-2 to AB-3) and 1.5 meV atom⁻¹ (AB-3 to AB-2). They also measured the lattice constants to be $9.46 \times 9.46 \times 6.75$ Å for AB-2 and $9.46 \times 9.46 \times 6.71$ Å for AB-3, indicating an interlayer spacing of 3.38 and 3.36 Å, respectively [14]. Zheng et al. [15] considered double layer configurations using supercells of $9.45 \times 9.45 \times 40$ Å; and also found the AB-2 and AB-3 stackings to be most stable, with the inter-layer distances of the two models being 3.42 and 3.40 Å, respectively.

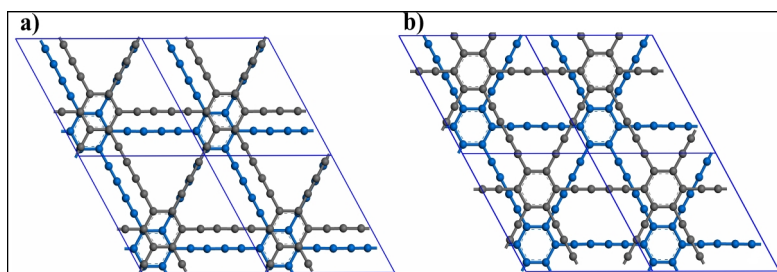


Figure 2: Schematic views of two layers of bulk GDY with (a) AB-2 and (b) AB-3 stackings. In each case a $2 \times 2 \times 1$ supercell is shown. Grey and blue balls represent carbon atoms. The two layers have been coloured differently to distinguish between them. The interlayer spaces are very similar (3.38 Å for AB-2 and 3.36 Å for AB-3).

The use of GDY as an anode material in LIBs has been demonstrated theoretically and computationally. Sun and Searles [16] used density functional theory (DFT) calculations to study the capacity for Li intercalation between GDY layers and the mobility of Li. They showed that the maximum adsorption capacity of GDY was LiC₃ (equivalent to 624 mA h g⁻¹), which is higher than the capacity of graphyne at LiC₄ (equivalent to 487 mA h g⁻¹) and graphene at LiC₆ (equivalent to 372 mA h g⁻¹) [16, 17]. In addition, they found that the most energetically favourable site for the Li atom was on the 18-carbon pore, but off-centre and near the corner of the pore. They also showed that the energy barriers for in-plane diffusion of Li (i.e. parallel to the GDY sheet) within the 18-carbon pore (corner to corner), from the 18-carbon pore to the 6-atom ring, from one pore to an adjacent pore and out-of-plane (i.e.

through the GDY sheet) were 0.18, 0.84, 0.70, 0.27 eV, respectively. The energy barrier for the path through the GDY sheet was found to be lower than that for movement of a Li from one 6-membered ring to another in graphene (0.32 – 0.34 eV, [18, 19]), indicating that the mobility of Li in bulk GDY could be greater than that in graphite.

Zhang et al. [20] also used DFT calculations to study the intercalation of Li in GDY. Similarly to Sun and Searles they found a capacity of LiC_3 for a GDY single layer. For the single layer, Zhang et al. considered a triangular placement of 3 Li atoms near the corners of each triangular pore and on the both sides of GDY single layer and calculated an average binding energy of 1.60 eV. We note that this is similar to the cohesive energy of Li, 1.630 eV [21], so these results indicate that clustering of Li atoms could occur. They also considered bulk GDY, with an AB stacking such that the centre of a hexagon on one layer is above the centre of the triangular pore for another. We note that this stacking is different from the four low energy stackings identified by Luo et al. [14]. For this bulk GDY, they predicted a loading corresponding to LiC_6 , with an average binding energy of 2.19 eV Li^{-1} . Further addition of Li to this structure resulted in buckling of the sheets. As well as the binding energies, Zhang et al. evaluated the energy barriers for Li diffusion on the GDY sheet: within the 18-carbon pore triangular pore; from the triangular pore to the 6-carbon hexagon; from one triangular pore to the adjacent one; and through the GDY sheet, finding energies of 0.13, 0.72, 0.51, 0.07 eV, respectively. The differences in the results obtained by Sun and Searles, and Zhang et al. can be accounted for by the different in methodology such as the size of the supercell and the treatment of van der Waals interactions, although we note that the trends are the same and the values within 0.2 eV of each other.

To test the utility of GDY in LIBs, Huang et al. [8] experimentally considered a Li intercalated GDY electrode and found a maximum reversible capacity of 520 mA h g^{-1} after 500 cycles at 500 mA g^{-1} , and 420 mA h g^{-1} after 1000 cycles at 2 A g^{-1} . They measured the interlayer distance of the GDY at 3.65 Å using scanning electron microscope (SEM) and transmission electron microscope (TEM) [8]. These experiments confirmed that GDY performs well as an electrode for LIBs.

Recently, Xu et al. [22] also carried out DFT calculations of Na binding to GDY and indicated that it should be a good candidate for an anode in NIBs. Using a similar methodology to Zhang et al. [20], they considered a number of symmetric loadings of Na on the GDY and concluded that the arrangement of 6 Na atoms close to the corners of a pore in a single layer is the most stable arrangement of those considered (NaC_3). They also found 3 Na atoms can be placed between layers of a unit cell in bulk GDY (with the same AB stacking considered by Zhang et al. [20]) to give a capacity corresponding to NaC_6 . In addition, they calculated the energy barriers for various transition pathways across and through a GDY sheet and found that the barriers for Na diffusion from near the corner of triangular pore to the 6-carbon hexagon, from one pore to adjacent pore in a direct pathway (in-plane) and from one side of the layer to other side in a perpendicular direction (out-plane) were 1.09, 0.64 and 4.5 eV, respectively. Clearly, as expected, these values are large compared to the barriers for diffusion of Li. The last value is for out-plane movement of Na at the corner of pore. This is unlikely to be the lowest energy path and therefore we will further explore if movement directly through the pore along another path might be possible.

The work of Xu et al. has provided important information on the binding of Na on single and bulk GDY, and diffusion on a single GDY sheet. In this manuscript we present additional results on these systems and also use DFT calculations to determine the maximum loading of Na on a single GDY sheet and bulk GDY. Furthermore, we carry out comprehensive calculations on the energy barriers for diffusion of Na across a GDY layer, and in-plane and out-of-plane diffusion between GDY layers in bulk systems. We demonstrate that both in-plane and out-of-plane diffusion should be possible in GDY. We also explain the observations by considering the charge density distribution, Bader charges and density of states (DOS) analysis.

2. Computational Methods

To study the interaction of Na with GDY, DFT calculations were performed as implemented in Vienna *ab initio* Simulation Package (VASP), version 5.3.5. The system is considered to be periodic in the three dimensions, and a plane-wave basis set is used. Within this package, the generalized gradient approximation (GGA) with projector-augmented wave (PAW) method was used. A Gaussian smearing with the smearing parameter, σ set to 0.05 was selected. To account for the van der Waals interactions, the DFT-D2 method of Grimme [23] was used. For calculations considering a single layer of GDY, the Brillouin zone was sampled with a $3 \times 3 \times 1$ k-point mesh and the bulk layers were sampled with $3 \times 3 \times 2$ k-point mesh, using the Monkhorst-Pack scheme. The cut-off energy for the plane-wave basis set was selected to be 1,000 eV, which is quite high due to the existence of single and triple bonds in the carbon chains of GDY which required a hard carbon PAW potential (C_h) to account the shorter bond length accurately. We also used the Na_sv potential for Na, which treats the 2p and 2s semi-core states as valence states leading to 9 valence states. The energy convergence criterion was selected to be 1×10^{-6} eV and the force convergence criterion was selected to be between 0.05 eV \AA^{-1} and 0.01 eV \AA^{-1} . The number of k-points and cut-off energy, force and energy convergence criteria were optimized in preliminary calculations.

In calculations of Na on the 2D GDY layer, a single GDY unit cell was used, and the optimized cell lattice parameters for the pristine GDY layer were determined to be $9.46 \times 9.46 \text{ \AA}$. A vacuum of 20 \AA above the layers was selected, which was shown to be sufficient to ensure that interactions between layers were small compared to the binding energies we obtain. For the bulk system calculations, a single GDY unit cell was also used and both the AB-2 and AB-3 stackings were considered. In both cases, full lattice optimizations of the a, b and c lattice parameters gave values of $9.46 \times 9.46 \times 6.58 \text{ \AA}$, corresponding to a GDY layer spacing of 3.29 \AA . We also considered different van der Waals corrections to Grimme's DFT-D2 scheme, [23] including vdW-opt88 and vdWopt86b, however like Klimeš [24] found almost the same lattice parameters as obtained using DFT-D2. We therefore used DFT-D2 vdW corrections in all our calculations for consistency. The transition state structures and their energies were determined using the Nudged Elastic Band (NEB) approach with the climbing image method [25] in conjunction with tangent definition given in [26].

After optimisation of the GDY 2D sheet and the bulk system, the maximum loadings were determined by adding Na to the materials while ensuring that the binding energy was higher than the cohesive energy of Na (which would result in clustering of the Na and inhibit its

mobility), and that the material did not become severely distorted. The binding energy between each Na atom and the GDY substrate is determined by:

$$E_b = \frac{E(GDY.Na_n) - nE(Na) - E(GDY)}{n} \quad (1)$$

where $E(GDY.Na_n)$, $E(Na)$ and $E(GDY)$ are the total energy values of GDY with n Na atoms adsorbed, the energy of Na as an isolated atom in gas phase, and the energy of GDY as standalone 2D sheet, respectively. Therefore a negative binding energy indicates that the binding is favourable. The theoretical electrical capacity of the anode material in mA h g^{-1} is:

$$E (\text{mA h g}^{-1}) = \frac{n_{Na}F}{3.6(n_{Na}m_{Na} + n_Cm_C)} \quad (2)$$

where m_{Na} and m_C are the atomic masses of the Na and C atoms in g, n_C and n_{Na} are the number of C and Na atoms in a unit cell and F is Faraday's constant, $9.648 \times 10^4 \text{ C mol}^{-1}$.

3. Results and Discussion

3.1. Na interaction with single layer GDY

In order to examine the strength and nature of the interaction of Na with GDY, the structures formed and the maximum likely loading of Na on GDY, we initially considered a single GDY sheet. Loadings of 1 – 9 atoms on the unit cell (18 carbon atoms) were considered. With each loading, all likely minimum energy structures were selected as initial configurations and the structures were optimized. The likely structures for systems with higher loadings were determined based on the low energy structures with lower loadings. Over 40 different initial configurations were considered overall. In all cases, the initial structures either had all Na atoms on one side of the GDY sheet, or in the plane of the sheet, although in some cases one or more Na atoms moved to the other side during optimization. One-sided or in-plane binding was considered since our ultimate aim is to look at bulk systems which, as a simplistic first approximation, can be considered as an assembly of single sheets with Na bound to one side. Loadings of more than 7 Na atoms on GDY either formed highly distorted structures or the Na atoms were located far from the GDY layer, so a loading of 7 was considered to be the maximum capacity. Figure 3 shows the average binding energies and corresponding structures for some of the systems considered. The upper curve connects the binding energies corresponding to the minimum energy structures at each loading that had a low level of distortion judged by examination of the structures, and their corresponding structures are shown above the curve. In addition, some energies and structures that resulted in distorted GDY are shown and connected by the lower curve. We note that the structures with visible distortion were often found to have stronger binding energies (more negative E_b); however, there is likely to be a large energy barrier for achievement of those configurations, and they might not be observed in experiment except under extreme conditions. Therefore we focus on the undistorted structures. As expected, the average binding energies of these configurations gradually decrease with an increase in Na loading.

The values of the average binding energies and average distance of the Na from the sheet for a number of the structures considered are given in Table 1. Energetically, the favourable structure obtained by adsorption of a single Na atom on the GDY sheet is with the atom in the plane of the sheet and at the centre of the pore. This position was more than 1 eV lower in energy than the position over the 6-carbon ring, and initial placements of the Na at different positions on the pore all resulted in this same minimum energy position. This conclusion is similar to that obtained by Xu et al., and is in contrast to the Li atom, which preferred to settle closer to the pore's corner [16, 20].

Our average E_b value for 6 atoms over the pores (-1.32 eV Na^{-1}) is similar to that reported value of Xu et al. at -1.30 eV Na^{-1} [22], and the structures and distances of the Na atoms from the sheet are also similar. However, we also found that 7 Na could be adsorbed on the sheet with a similar average binding energy and distance between the Na atoms and the sheet. In this case, as well as three Na near the corners of the triangular pore, one was situated above the 6-carbon ring, and the average binding energy was found to be -1.32 eV Na^{-1} . The ability of a Na atom to bind above the 6-carbon ring is consistent with the calculated binding energy of a single Na above the 6-carbon ring of -1.48 eV Na^{-1} (see Table 1). Therefore, our calculations indicate that the maximum Na capacity of GDY for Na_7C_{18} or $\text{NaC}_{2.57}$ with the Na atoms situated above the sheet (at a distance of $d_{\text{ad}} \approx 2.0 \text{ \AA}$), equivalent to theoretical electrical capacity of 497 mA h g^{-1} .

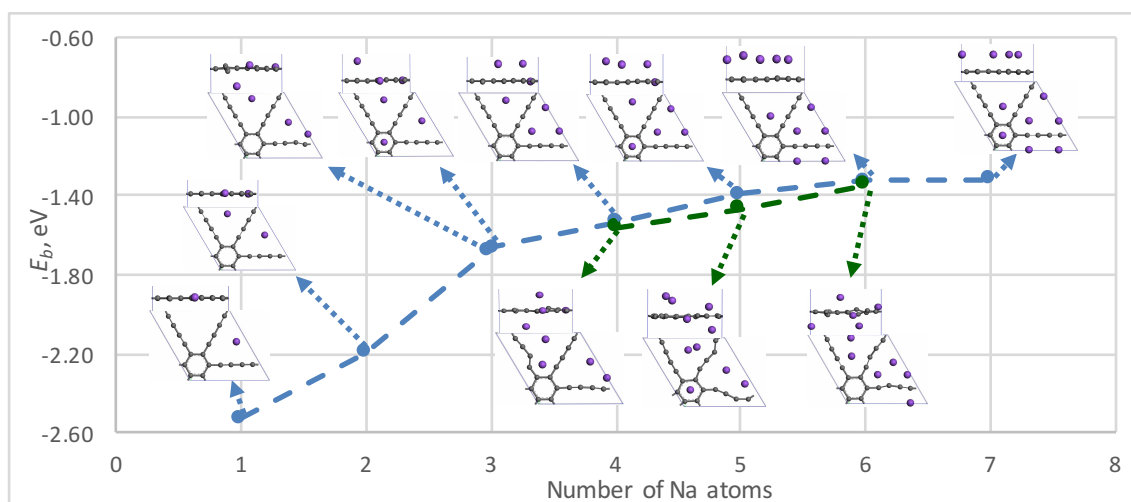


Figure 3. Binding energy as a function of the number of Na atoms on a single GDY sheet. The grey balls represent carbon and the purple balls sodium. Top and side view of the structures are shown. The blue diamonds show binding energies for the undistorted structures and the green diamonds shown binding energies for distorted structures. The lines serve as guides to the eye.

Table 1. Average binding energies and distances of Na on a single GDY sheet.

Na atoms per unit cell	Position	Average Na-GDY distance d_{ad} (Å)	Strongest E_b (eV per Na atom)	Strongest E_b (eV per Na atom) – undistorted configuration
1	Over hexagonal ring	1.77	-1.479	-1.479 ^a
1	Centre of triangular pore	0.0	-2.527	-2.527 ^a
2	Centre of two triangular pores	0.0	-2.196	-2.196 ^a
3	Centre of two triangular pores and over ring	0.0, 2.24	-1.683	-1.666
4	One at centre of pore and three over another pore	variable	-1.563	-1.538
5	One over ring, one at centre of pore and three over another pore	variable	-1.466	-1.391
6	Three over each pore	~ 2.0	-1.347	-1.324
7	Three over each pore and one over ring	~ 2.0	-1.317	-1.317 ^a

^a In these cases, the configuration with the most strongly bound Na was not distorted

3.2 Na intercalation in bulk GDY

Na intercalation between the GDY bulk layers was considered by studying a unit cell with two GDY layers, which was periodic in all dimensions, and with lattice vectors set to be those of the optimized bulk GDY. We considered AB-2 and AB-3 stackings of the GDY layers (see figure 2), but in this section we focus on the results of the AB-2 stacking due to its low energy and the large pore that is formed perpendicular to the GDY sheets, which we anticipated would be most easily able to accommodate a Na atom. We note that this differs for the work by Xu et al. [22] who also considered two layers in a periodic cell, but a different stacking. It also differs in that they allowed variation of the lattice vectors on loading, so allowed the system to expand if required. The real experimental system will be intermediate between these, with expansion being restricted by the surroundings, and we discuss this further in another section. The optimized length of the cell in the direction perpendicular to the sheets was 6.58 Å, giving an interlayer distance of 3.29 Å which can be compared with the experimental value of 3.65 Å [8]. The small differences between our result and other calculated results by Zheng et al. [15] (3.42 Å for bi-layer AB-2 GDY), Luo et al. [14] (3.38 Å for bulk AB-2 GDY) and Xu et al. [22] (3.5 for bi-layer GDY) are likely to be due to the method used for van der Waals interactions (see a comparison of different methods in [14]). We note that this interlayer distance is very similar to that observed in graphite, and if the

bulk material is able to accommodate Na it must therefore be due to the existence of large pores and the space created due to the stacking of the layers.

As in the case of the single GDY sheet, Na atoms were added to the unit cell at all likely initial positions and the structures were optimized. A loading of 1 to 12 Na atoms per unit cell (which contains 36 C atoms) was considered. Over 25 different initial structures were selected. Figure 4 shows the average binding energies and corresponding structures for some of the bulk systems considered, as a function of the number of Na atoms in the unit cell. A blue dashed line connects the binding energies of systems where little distortion of the structure is evident, whereas a green dotted line connects the strongly binding distorted structure energies. Structures of the distorted configurations have been placed below the lines, and undistorted configurations above the lines. In addition, Table 2 gives E_b and the average distance between the Na atoms and the closest sheet, for various loadings.

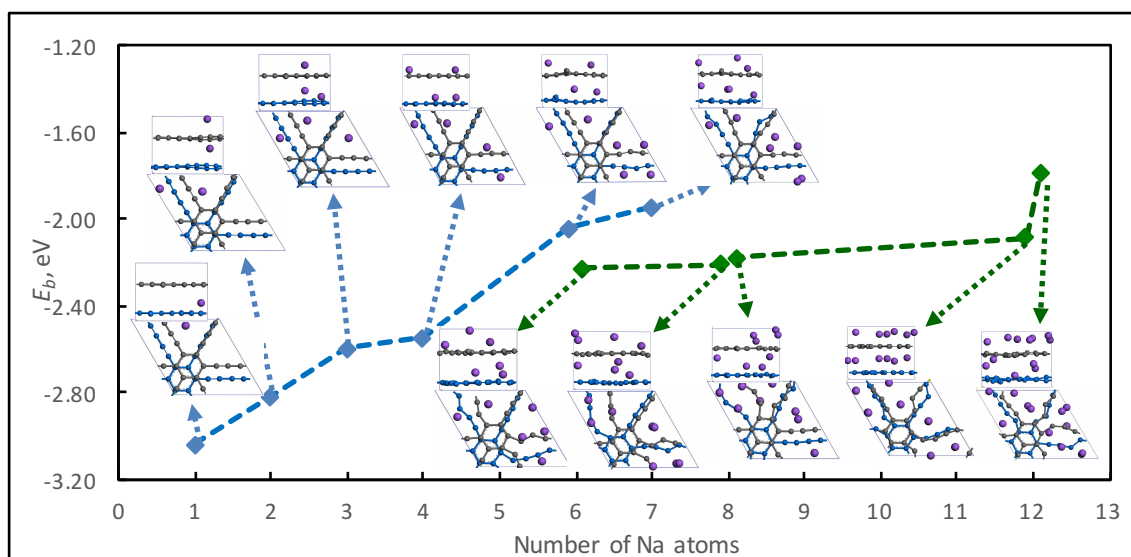


Figure 4. Binding energy as a function of the number of Na atoms intercalated in bulk GDY. Grey and blue balls represent carbon atoms. The two layers have been coloured differently to distinguish between them. Purple balls represent sodium. The top and the side view of each structure are shown. The blue diamonds show binding energies for the undistorted structures and the green diamonds shown binding energies for distorted structures. The lines serve as guides to the eye.

All the E_b values obtained have a magnitude larger than 1.113 eV (cohesive energy of Na), so no clustering of Na atoms is expected for the systems shown, and indeed this is not observed in the structures. Although a maximum loading of 12 Na atoms in the unit cell was considered, after 7 atoms all the initial structures considered became significantly distorted. As noted, we did not allow the bulk material to expand on addition of Na for the systems shown in figure 4, however this possibility is also considered later in this manuscript. Overall, our results suggest that the maximum Na capacity of bulk GDY without significant distortion and without expansion of the supercell is Na_7C_{36} or $\text{NaC}_{5.14}$, equivalent to 316 mA h g^{-1} . We note that the single GDY layer had a capacity of Na_7C_{18} or $\text{NaC}_{2.57}$, which is twice that of the prediction for bulk GDY. This is due to the size of the pore, since in the single

sheet case higher loadings involved Na atoms located about 2 Å above the sheet, which is more than half the interlayer spacing in bulk GDY. However, the loading obtained for bulk GDY is more likely to be representative of the bulk loading that can be attained. Furthermore, a capacity of 316 mA h g⁻¹ is comparable to existing materials, and if the mobility is high will make bulk GDY a interesting material for consideration as a Na battery anode. This will be explored in the next section.

Table 2. Binding energy values for Na intercalation on the GDY bulk layers with AB-2 stacking

Na atoms per unit cell	Strongest E_b (eV per Na atom)	Strongest E_b (eV per Na atom) – undistorted configuration
1	-3.04	-3.04
2	-2.82	-2.82
3	-2.60	-2.60
4	-2.55	-2.55
6	-2.23	-2.05
7	-1.95	-1.95
8	-2.21	NA
12	-2.09	NA

We also observe that, in contrast to the single layer cases where the Na atoms have minimum energy structures with the Na atom in the plane of the GDY sheet, in the bulk cases Na atoms tend to be between the layers, even when there is only a single Na atom. We will later demonstrate that there is little change in the potential energy as the Na moves between the sheets along an appropriate path. Finally, the very slightly distorted configuration of 6-Na atom in figure 4 (on the blue curve) is of significance since it corresponds to a case where 3 atoms are placed near the corners of each pore, forming a symmetric conformation. This structures is similar to that obtained with 6 Li and Na atoms placement on double layers of GDY, in the works of Zhang [8] and Xu [9], respectively.

For the AB-3 stacking, the single Na atom in GDY has minimum energy structure with the Na located at very similar site as in the case for a single Na atom in GDY with AB-2 stacking (see the Supplementary Materials, figure S1), and the Na atom has a binding energy of -3.01 eV which is also similar to the result for the AB-2 stacking. The energy for the system with the Na atom in the plane of the membrane is just 0.05 eV higher.

3.3 Energy barriers for transitions across, and through, GDY.

In this section, we present calculated energy barriers for Na movement across GDY layers in GDY single sheet and bulk systems. The energy barriers determine the mobility of the Na, and therefore affects the charge and discharge rates in a battery. Either single point calculations along a desired trajectory, or NEB calculations were used to determine the energy barriers and configurations at the transitions state. To give an idea of the magnitude of the energy barriers, we can compare them with those for hopping of a Li between rings of

graphene of 0.32 eV [18], in graphite of 0.34 eV [19], and the barrier for movement of Li from one pore to another in GDY of about 0.51 eV [20], 0.70 eV. [16]

For the single GDY sheet, we consider three pathways between local and global minima which are presented in figure 5. The energy barriers and distance of the Na atoms from the GDY sheet are summarized in Table 3. Figure 5a shows the transition from a Na atom at the centre of the triangular pore (and in the plane of the GDY sheet) to a Na above the centre of the 6-carbon ring. At the transition state, the Na atom is directly above a carbon-carbon bond of the 6-carbon ring. The energy barrier for movement of the Na atom from the pore to the ring is relatively large at 1.17 eV and therefore this transition will be unlikely under typical conditions. There is also a barrier for movement from the ring to pore of 0.13 eV, but it is relatively low and therefore it is anticipated that the Na will move off the ring to the pore quite readily. These values are similar to those obtained by Xu et al. (1.09 eV and 0.18 eV).

The second pathway was between the centres of two adjacent pores is shown in figure 5b. The initial and final positions are global minima and it is found that the Na will move across the middle of the 4-carbon chain with a barrier of 0.80 eV. This value is larger than the hopping energy of Li on graphene, and similar to the barrier for transition between the triangular pores of GDY for Li. It is comparable with the result of Xu et al. who found a barrier of 0.64 eV using a different methodology. This barrier is smaller than that for movement from the centre of the triangular pore to the 6-carbon ring, and therefore this is a more likely pathway.

In both the cases described above, situations where there is a single Na atom in the supercell were considered. In the third case (see figure 5c), one Na atom was fixed at the global minimum at the centre of the triangular pore, and another was situated above the same pore such that the overall structure was a local minimum, and there are two Na atoms in the supercell. The barrier for movement of the second Na atom to the centre of the adjacent pore was found to be just 0.039 eV (see figure 5c and Table 2), with a transition state over the carbon chain, and therefore this Na would be very mobile. The barrier for the reverse pathway is moderate at 0.47 eV, and is much smaller than the barrier for movement of the Na at the centre of the pores when there is only one Na in the supercell. Therefore as the loading increases, the mobility of the Na is likely to become greater. As can be seen from figure 3, at low loading the Na tends to be situated at the very stable position at the centre of the triangular pore, but as loading increases the Na atoms are more likely to be situated out of the plane and this will also enhance mobility.

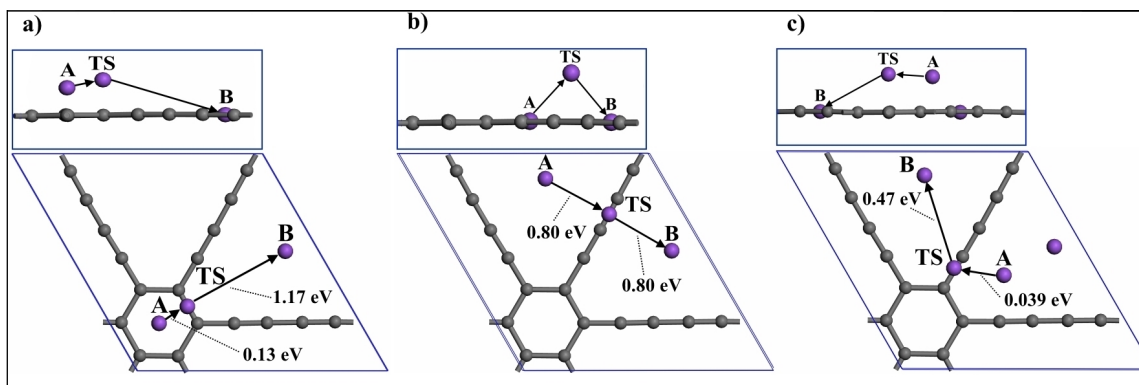


Figure 5. Transition states for movement of a Na across the GDY single sheet (a) between the ring and pore, (energy barrier from A to TS: 0.13 eV, from TS to B: 1.17 eV); (b) from one pore to another, (energy barrier from A to TS: 0.80 eV, from TS to B: 0.80 eV); and (c) from one pore to another in the presence of another Na atom (energy barrier from A to TS: 0.039 eV, from TS to B: 0.47 eV). The top and side view of the pathway are shown. Grey balls represent carbon and purple balls represent sodium atoms.

Table 3. Values of energy barriers for Na movement for 3 different pathways and distance of the Na atom from the GDY surface.

Transition	Na-GDY distance, d_{ad} (Å)			Energy barrier (eV)	
	Initial State (A)	Transition State (TS)	Final State (B)	Initial to Final State	Final to Initial State
See 5a	1.77	2.26	0.00	0.13	1.17
See 5b	0.00	2.16	0.00	0.80	0.80
See 5c	2.10	2.25	0.00	0.039	0.47

Finally, for the GDY sheet, we can consider the energy profile as an Na atom moves directly through the centre of the GDY plane. Because the Na is at a minimum energy position in the plane, there is an energy barrier in this direction which is equal to binding energy, 2.53 eV and therefore is quite high.

To judge if GDY is suitable for use as an electrode, it is important to consider the mobility of Na in bulk GDY. This is particularly true for the Na/GDY system because the lowest energy state changes from being in the plane of the GDY for the sheet, to between the pores for the bulk and therefore the energy barriers, pathways and mobility will change. In addition, at high loading the Na atoms are about 2 Å above the single sheet whereas the gap between the GDY sheets is only about 3.3 Å.

Firstly we consider the AB-2 stacking. This was selected due to the large pore perpendicular to the plane of the GDY sheet (see figure 2a), which we anticipated could provide a passage with relatively low energy barriers. However, this needed to be tested, especially in light of the large binding energy for Na at the centre of the GDY triangular pore, the known extremely high energy barrier for diffusion through the 6-carbon rings of graphene and the result of Xu

et al. [22] who showed that there is a very large barrier (4.5 eV) to out-of-plane movement through a pore of the single layer sheet, at a position close to the corner of the triangular pore.

We tested two pathways for movement within the interlayer gap of GDY with AB-2 stacking, between the GDY layers, and one for movement between the planes shown in figure 6a-c. Unlike in the single layer case, the binding energy of a Na atom did not vary greatly over a large region between the overlapping triangular pores. In fact many local minima were identified in this region, with energy differences of only approximately 0.05 eV using force convergence criterion of 0.01 eV \AA^{-1} . Furthermore, using a force convergence criterion of 0.05 eV \AA^{-1} gave results differing consistently in binding energy from those with 0.01 eV \AA^{-1} by about 0.17 eV. We therefore estimate the global minima energies for the bulk system to have errors of up to approximately 0.1 eV.

In figure 6a we show the pathway for a single Na between the layers from a minimum energy position on one pore to another on an adjacent pore, passing between the 4-carbon chains that lie directly above each other in the AB-2 stacking. There is a very high energy barrier of 2.2 eV due to the proximity of the Na to the carbon chains at the transition state. At that point, the carbon chains are distorted to accommodate the Na atom, and the average distance between the two sheets increases by about 8.5%, however the strong bonding in the chain prevents too much distortion, developing strain in the chain that contributes to the large energy barrier. The size of the energy barrier indicates that in the bulk system, movement of a Na atom between the chains is highly unlikely under standard operating conditions. The small difference in the energy barriers is due to slightly different initial and final geometries.

The second pathway, which is shown in figure 6b, is between the layers from a minimum energy position on one pore to another on an adjacent pore, but in this case it passes between the two 4-carbon chains that do not lie directly above each other. The transition state is mid-way between the chains and some distortion of the chains is observed, however these carbon chains are 4.69 \AA apart when the Na is not present, making space for the Na to move and the energy barriers are greatly reduced to 0.82 and 0.84 eV. This value is similar to the barriers observed for movement across the carbon chains in the single GDY sheet.

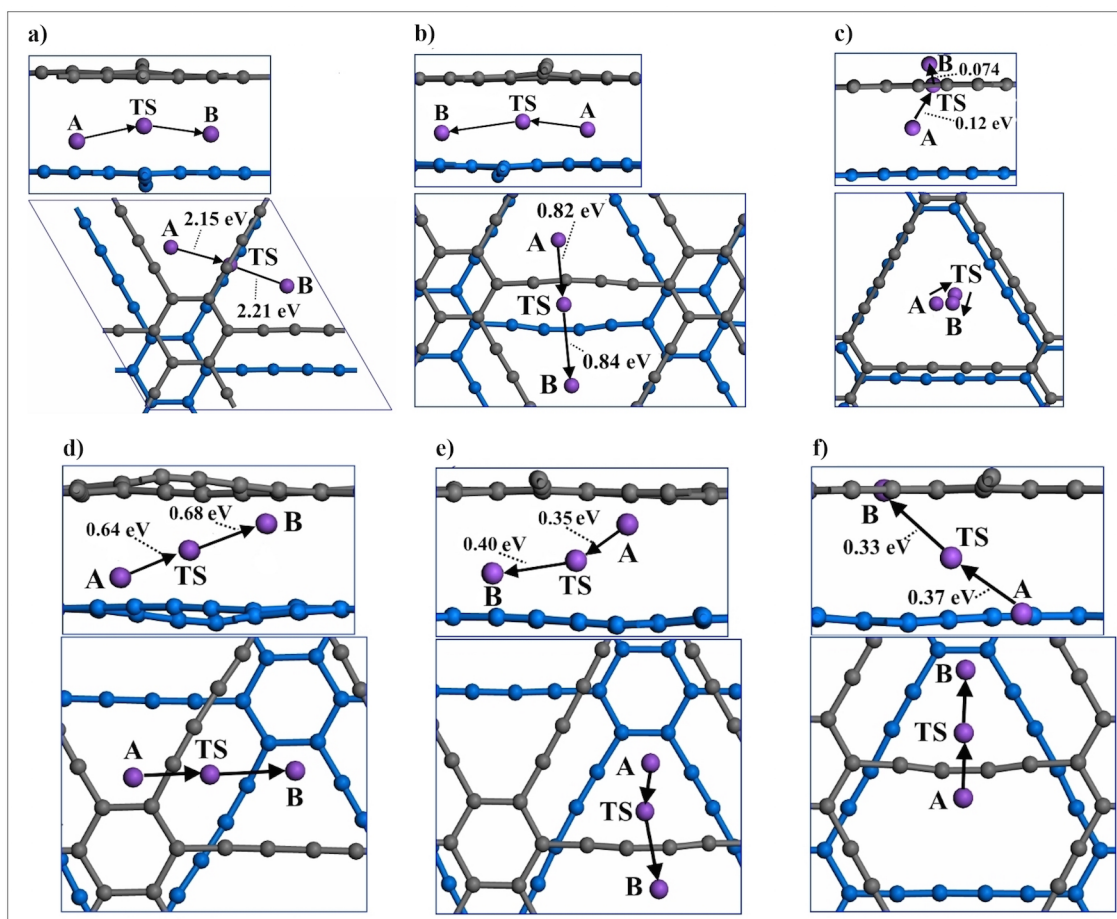


Figure 6. Transitions state for movement of a Na atom in bulk GDY with (a)-(c) AB-2 stacking and (d)-(f) AB-3 stacking. (a), (b) are pathways between GDY layers and (c) is through a GDY layer. The top and side view of the movement are shown. (d) and (e) are both paths between layers and (f) is for a path from the centre of a pore on one layer to the centre of a pore on another layer. The top and side view of the pathway are shown. Grey and blue balls represent carbon atoms in different layers to distinguish between layers. Purple balls represent sodium atoms.

The third transition studied was through the GDY sheet, from a minimum energy position at the centre of a pore, through the sheet to a minimum energy position on the other side of the sheet. The barriers for the forward and reverse paths were both low: 0.12 eV and 0.074 eV, respectively. These values are both smaller than the hopping of Li between rings on graphene and only $\sim 5k_B T$ and $3k_B T$ at 298K, so would be expected to be easily overcome. This result is very encouraging for the use of AB-2 stacked GDY in NIBs.

Attempts to find transitions states in the pathway from one side of the slit pore formed by the two sheets to the other were problematic due to the very flat potential energy surface in this region. Therefore in order to get an idea of the energy landscape across the pore, single point energies were calculated along a zig-zag path that connected to the local minima at the centre of the slit pore, and the local minima in the plane of the sheet. The results are shown in figure 7. Clearly the barriers are very low.

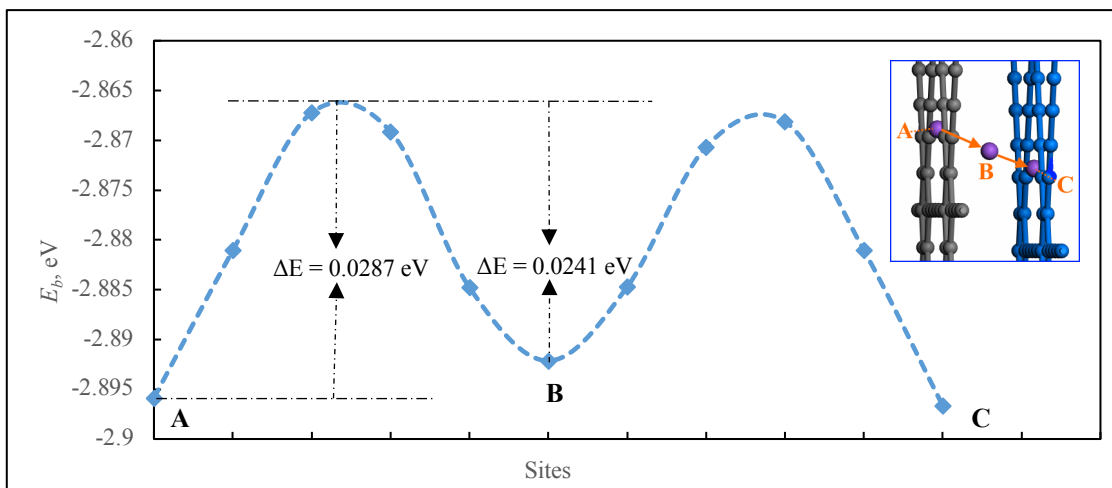


Figure 7. Energy profile for movement of an Na atom through bulk GDY, from minimum energy positions at the centres of the pores. The position of the Na atom at sites A, B and C is shown in the inset.

Due to the very low energy barriers perpendicular to the sheets in the AB-2 stacked GDY, and the moderate energy barriers parallel to the sheet, across the carbon chains the diffusion would be predominantly through the triangular pores (so one-dimensional). This is not ideal as blockages are more likely to prevent diffusion. For this reason, AB-3 stacked GDY was also considered. As discussed above, AB-3 stacked GDY has very similar stability to AB-2, and has been predicted to be more stable [14]. Due to the greater distance between the 4-carbon chains and poorer alignment of the triangular pores in AB-3 GDY, we would expect the barriers parallel to the sheet to be reduced, and those perpendicular to the sheet to be increased.

Again, the potential energy surface between the triangular pores is very flat, so many local minima were identified and the results are sensitive to the selection of the force convergence criterion. Two significant pathways for transition of a Na atoms within the interlayer spacing are shown in figure 6d-e. In figure 6c, the transition is from a minimum energy position located above a triangular pore on one sheet, between two 4-carbon chains, to a similar minimum energy position in an adjacent triangular pore of the sheet on the other side. The energy barrier of approximately 0.68 eV in this case is lower than any of the transitions within the interlayer spacing observed with an AB-2 stacking.

The second transition pathway is shown in figure 6e. In this case, the initial position is similar to the final position in 6d, but passes over a single carbon chain to reach a final position is close to the sheet on the other side of the slit formed by the two pores. The energy barrier for this is just 0.35 eV, and for the reverse pathway is 0.40 eV. These barriers are quite similar to those for Li hopping on graphene, and therefore we anticipate that such a diffusion path would be likely in a NIB.

In figure 6f, the pathway from a position at the centre of one pore, in the membrane plane to the centre of another pore in the plane of the adjacent membrane is shown. The barriers in this case are 0.37 and 0.33 eV, showing that the barriers for movement from one plane to

another are sufficiently low that this is likely to occur. Clearly using the pathways shown in figure 6f zig-zag pathways could be constructed with a barriers of approximately 0.37 eV.

According to the Luo et al. [14], the AB-3 and AB-2 stackings are convertible to each other with a maximum barrier of energy of 1.5 meV atom⁻¹, which is quite low. Hence the two configurations can coexist in real experiment. These results indicate that the barriers for diffusion are low, even with a cell that is not able to expand. In addition the loadings that can be obtained are high, making this a very promising material for NIBs.

3.5 Expansion of bulk GDY due to loading with Na

So far all calculations of loading and diffusion have been done with the lattice parameters fixed. On loading, if there is insufficient space for a Na atom in an interlayer spacing, the slit pore might expand to accommodate it. As in our simulated bulk systems we have two inequivalent slit pores in the simulation cell, there was some freedom for one pore to expand, and expansion of up to about 5.5 % was observed with a loading of 7 Na atoms. This would lead to contraction of the other spacing and therefore it is somewhat contained. Here we consider what expansion might occur if there is no restriction on the lattice parameters. The results presented here are for an idealized situation where the loading is uniform and bulk GDY is free to expand. As mentioned above, real systems will be an intermediate between the restricted case considered above and that considered here. Of course, the mobility within a slit pore will be even greater if the lattice parameter is allowed to increase.

In order to look at the degree of expansion that might be expected, we considered a number of loadings of the AB-2 stacking system. In all cases except one (described below) we took the minimum energy, undistorted structures shown in figure 4, and incrementally changed the lattice parameter by 1%, re-optimising the structure at each stage and calculating the energy of the system. We found that when 1 Na atom is placed above each of the triangular pores in the unit cell (4 atoms in total or NaC₉), the interlayer spacing contracts by 1% to 3.26 Å. This suggests that each Na is binding to both surfaces of the slit pore containing it, and that this is a very stable system. As the loading increases we see expansion of the interlayer spacing, and when 7 Na atoms are inserted (Na₇C₃₆), giving the maximum capacity indicated above (see configuration in figure 4), the lattice spacing is optimal with at 12% expansion of the layers (3.29 Å to 3.69 Å). In addition, the binding energy increased from -1.95 to -2.07 eV atom⁻¹. To incorporate 14 Na atoms in the unit cell, we placed the Na atoms on each sheet in a configuration corresponding to the loading of a single GDY sheet with 7 Na shown in figure 3, and then allowed the sheets to gradually come together. In this case the GDY sheets did not distort greatly and an expansion of 28% was observed with a binding energy of -1.80 eV atom⁻¹.

These results indicate that a loading of much greater than Na₇C₃₆ (i.e. Na₁₄C₃₆) could be obtained when if expansion is allowed, which is equal to the loading obtained with the single sheet. This is similar, but slightly higher, than the loading observed by Xu et al. [22] which might be attributed to a different selection of initial configurations, the computational parameters used and/or the different stacking considered. It shows that the calculations that

we have carried out on the bulk system are the worst case predictions, and give further indication that a GDY NIB is a promising alternative to existing rechargeable batteries.

3.6 Charge density, Bader and DOS analysis

In order to provide a deeper understanding of the binding between the Na and GDY and the nature of the material formed by adsorption of Na on GDY, we have carried out charge density calculations, Bader and DOS analyses.

Figure 8 presents charge density difference isosurfaces, $\Delta\rho = \rho_{GDY Na} - \rho_{GDY} - \rho_{Na}$ where ρ is the charge density of the combine or separated systems, when 1, 3 and 7 Na atoms are placed on the unit cell of the GDY sheet. In all cases there is a clear transfer of charge from the Na to the GDY sheet, with the red colour indicating an electron deficient isosurface ($\Delta\rho = -0.0012 e \text{ \AA}^{-3}$), and the blue colour indicating an electron rich isosurface ($\Delta\rho = 0.0012 e \text{ \AA}^{-3}$). When 1 or 3 atoms are placed on the surface, the electron transfer from the Na atoms is quite localized although the electrons are distributed to all bonds of the GDY sheet. The isosurface is between the Na atom on the 6-carbon ring and the ring, indicating the charge on that Na atom is lower than those over the triangular pore. As the number of Na atoms increases to 7 Na, the region of electron depletion becomes more widely distributed; and the electron rich region remains around the carbon chains and ring.

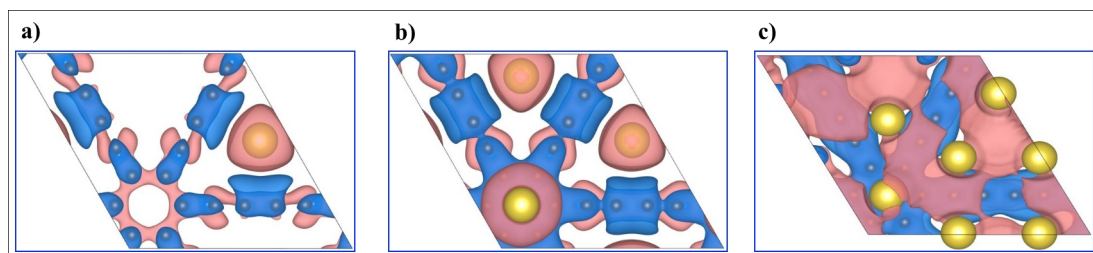


Figure 8. Charge density difference for (a) GDY Na₁, (b) GDY Na₃, and (c) GDY Na₇. The red colour indicates an electron deficient isosurface ($\Delta\rho = -0.0012 e \text{ \AA}^{-3}$) and the blue colour indicates an electron rich isosurface ($\Delta\rho = 0.0012 e \text{ \AA}^{-3}$).

In order to further characterize the degree of charge transfer, a Bader charge analysis [27, 28] was carried out for each of these systems. In all cases the charge on the carbon atoms was similar for each carbon. When 1 Na atom was present, its Bader charge was +0.81. When 3 Na atoms distributed as in figure 8b), the two Na atoms on the pore have Bader charges of +0.81 but that on the ring has a charge of +0.59, indicating that the charge transfer for the Na atom over the ring is lower. For the case when 7 Na atoms were adsorbed, the charge transfer from each of the Na atoms was reduced with 4 of the atoms on the pore having a charge of +0.45 to +0.46 and the other 2 on the pore having a charge of +0.25 to +0.26. The Na on the ring has a small charge transfer with a Bader charge of +0.01. Although the sum of the charges on the Na atoms increases with the loading, the average charge on each does not due to the limit on the capacity of the GDY to accept electrons.

Finally, insight into the change in the electronic properties of pristine GDY due to adsorption of Na is given by consideration of the DOS (Density of States) analysis of pure GDY, GDY Na₁ and GDY Na₇. The results indicate that pure GDY has a small band gap of 0.37 eV, in agreement with previous results obtained using PBE functionals, [14], and suggesting that it has a semiconducting behaviour. However the insertion of Na atoms introduces states within the band gap transforming it into a metallic system (see figure S2 in the Supplementary Materials). The partial DOS was also carried out in each of these cases (see figure S3 of the Supplementary Materials).

4. Conclusion

In conclusion, we propose that Na on GDY is potentially a suitable anode for rechargeable batteries. Na is cheaper and more abundant than Li, and GDY provides large pores and space for a Na to intercalate in and then move throughout. According to the results, the maximum capacity of GDY for Na atoms is NaC_{2.57} for a single GDY layer (equivalent to 497 mA h g⁻¹), and NaC_{5.14} for GDY bulk layers (equivalent to 316 mA h g⁻¹) if we do not allow expansion of the GDY bulk unit cell. If expansion is allowed then this capacity is likely to increase to NaC_{2.57}. We have provided the first calculations of the energy barriers for transitions of Na between sites in the bulk GDY. The results indicate that Na atoms would readily move through the triangular pores normal to the GDY sheets in bulk GDY with an AB-2 stacking, and that they would readily move in directions both parallel and normal to the GDY sheets with an AB-3 stacking. Barriers are either lower or similar to those observed for Li on graphene.

5. Acknowledgements

The authors thank the Australian Research Council for support of this project through the LIEF program. This research was undertaken with the assistance of resources provided at the NCI National Facility systems at the Australian National University through the National Computational Merit Allocation Scheme supported by the Australian Government, from the Queensland Cyber Infrastructure Foundation (QCIF) and the University of Queensland Research Computing Centre. AFN also acknowledges support from the Australian Government through an Australian Government Research Training Program Scholarship.

6. References

- [1] S. Goriparti, E. Miele, F. De Angelis, E. Di Fabrizio, R. Proietti Zaccaria, C. Capiglia, J. Power Sources, 257 (2014) 421-443.
- [2] J.W. Fergus, J. Power Sources, 195 (2010) 939-954.
- [3] B. Scrosati, J. Garche, J. Power Sources, 195 (2010) 2419-2430.
- [4] M. Sawicki, L.L. Shaw, RSC Adv., 5 (2015) 53129-53154.
- [5] <http://www.faradion.co.uk> accessed October 21, 2016.
- [6] <http://aquionenergy.com> accessed October 21, 2016.
- [7] A. Blackman, Chemistry, John Wiley & Sons, Milton, Qld, 2012.
- [8] C. Huang, S. Zhang, H. Liu, Y. Li, G. Cui, Y. Li, Nano Energy, 11 (2015) 481-489.

- [9] Y. Cao, L. Xiao, M.L. Sushko, W. Wang, B. Schwenzer, J. Xiao, Z. Nie, L.V. Saraf, Z. Yang, J. Liu, *Nano. Lett.*, 12 (2012) 3783-3787.
- [10] D.A. Stevens, J.R. Dahn, *J. Electrochem. Soc.*, 147 (2000) 1271-1273.
- [11] M.S. Balogun, Y. Luo, W.T. Qiu, P. Liu, Y.X. Tong, *Carbon*, 98 (2016) 162-178.
- [12] D. Kundu, E. Talaie, V. Duffort, L.F. Nazar, *Angew. Chem. Int. Ed. Engl.*, 54 (2015) 3431-3448.
- [13] V. Palomares, P. Serras, I. Villaluenga, K.B. Hueso, J. Carretero-González, T. Rojo, *Energy Environ. Sci.*, 5 (2012) 5884-5901.
- [14] G. Luo, Q. Zheng, W.-N. Mei, J. Lu, S. Nagase, *J. Phys. Chem. C*, 117 (2013) 13072-13079.
- [15] Q. Zheng, G. Luo, Q. Liu, R. Quhe, J. Zheng, K. Tang, Z. Gao, S. Nagase, J. Lu, *Nanoscale*, 4 (2012) 3990-3996.
- [16] C. Sun, D.J. Searles, *J. Phys. Chem. C*, 116 (2012) 26222-26226.
- [17] H.J. Hwang, J. Koo, M. Park, N. Park, Y. Kwon, H. Lee, *J. Phys. Chem. C*, 117 (2013) 6919-6923.
- [18] K.T. Chan, J.B. Neaton, M.L. Cohen, *Phys. Rev. B*, 77 (2008) 235430.
- [19] F. Valencia, A.H. Romero, F. Ancilotto, P.L. Silvestrelli, *J. Phys. Chem. B*, 110 (2006) 14832-14841.
- [20] H. Zhang, Y. Xia, H. Bu, X. Wang, M. Zhang, Y. Luo, M. Zhao, *J. Appl. Phys.*, 113 (2013) 044309.
- [21] C. Kittel, *Introduction to Solid State Physics*, John Wiley & Sons, New York, 2004.
- [22] Z. Xu, X. Lv, J. Li, J. Chen, Q. Liu, *RSC Adv.*, 6 (2016) 25594-25600.
- [23] S. Grimme, *J Comput Chem*, 27 (2006) 1787-1799.
- [24] J. Klimeš, D.R. Bowler, A. Michaelides, *J. Phys. Condens. Matter*, 22 (2010) 022201.
- [25] G. Henkelman, B.P. Uberuaga, H. Jónsson, *J. Chem. Phys.*, 113 (2000) 9901-9904.
- [26] G. Henkelman, H. Jónsson, *J. Chem. Phys.*, 113 (2000) 9978-9985.
- [27] M. Yu, D.R. Trinkle, *J. Chem. Phys.*, 134 (2011) 064111.
- [28] W. Tang, E. Sanville, G. Henkelman, *J. Phys. Condens. Matter*, 21 (2009) 084204.

Sodium-intercalated bulk graphdiyne as an anode material for rechargeable batteries – Supplementary Materials

Amir Farokh Niaei¹, Tanveer Hussain¹, Marlies Hankel¹ and Debra J. Searles^{1,2,*}

¹ *Centre for Theoretical and Computational Molecular Science, Australian Institute for Bioengineering and Nanotechnology, The University of Queensland, Brisbane, QLD 4072, Australia*

² *School of Chemistry and Molecular Biosciences, The University of Queensland, Brisbane, QLD 4072, Australia*

*Corresponding Author

Debra J. Searles

Australian Institute for Bioengineering and Nanotechnology

The University of Queensland

Brisbane, QLD 4072, Australia

Telephone: +61 7 33463939

Fax: +61 7 3346 3992

Email: d.bernhardt@uq.edu.au

The minimum energy structure of AB-3 stacked GDY with a single Na atom per unit cell is shown in figure S1. In figure S2, the total density of states for a single layer of GDY with two different Na loadings is compared with pristine GDY, and in figure S3 the partial density of states for the system of 1 Na atom on a single GDY layer is shown.

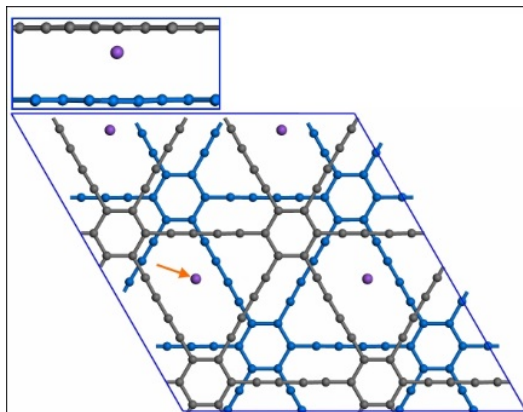


Figure S1. Minimum energy structure of a supercell ($2 \times 2 \times 1$ unit cells) of bulk GDY with AB-3 stacking, intercalated with 1 Na atom per unit cell (indicated by the orange arrow). The binding energy of the Na atom to the GDY, E_b , is -3.01 eV. Grey and blue balls represent carbon atoms with the different colours used to distinguish between the layers. Purple balls represent sodium atoms. The inset shows a side view of part of the supercell.

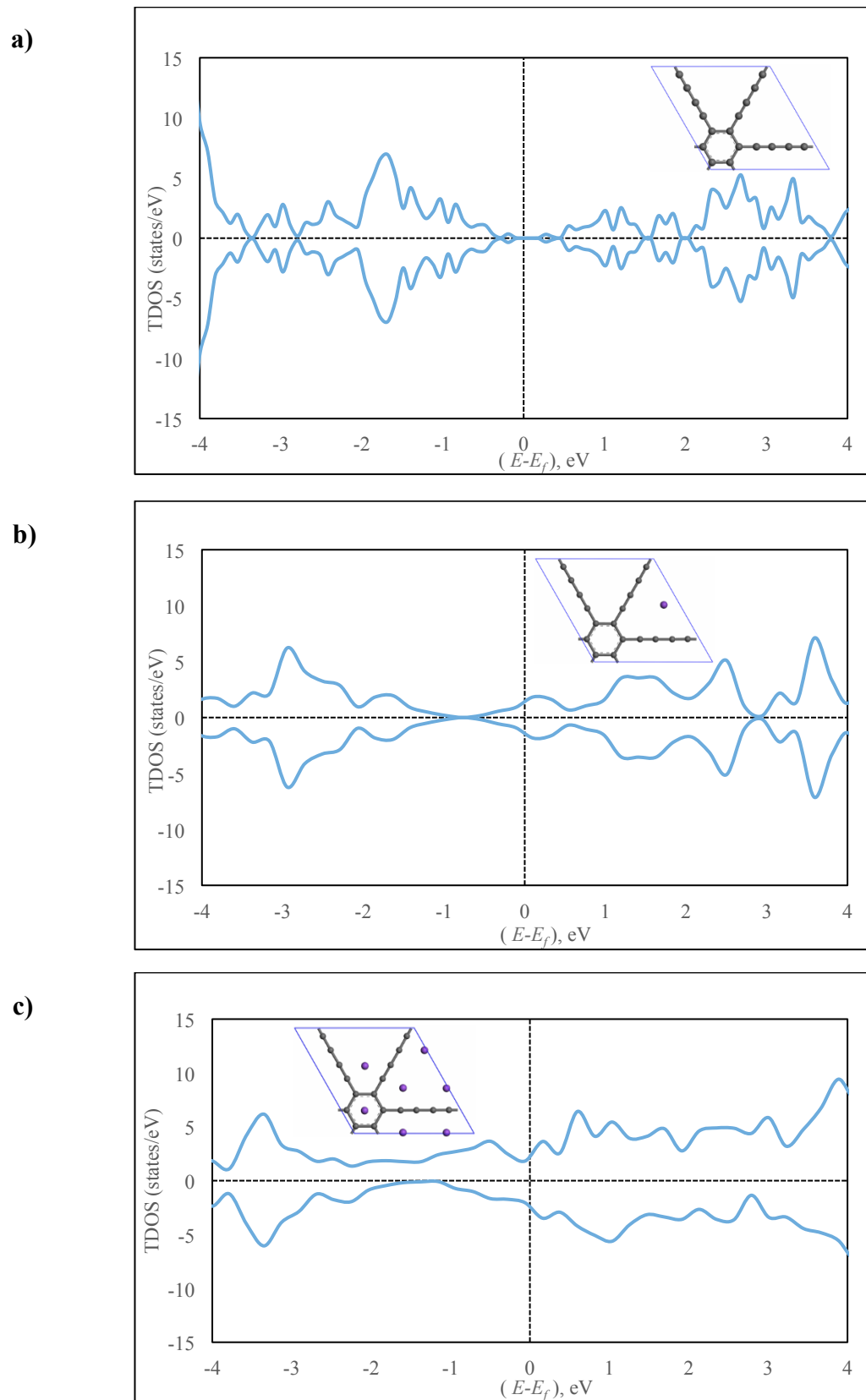


Figure S2. Total density of states (TDOS) for (a) pure GDY, (b) GDY Na and (c) GDY Na₇. The insets show the structures considered with C atoms represented by grey balls and Na atoms by purple balls. The energy shown is relative the Fermi energy, E_f .

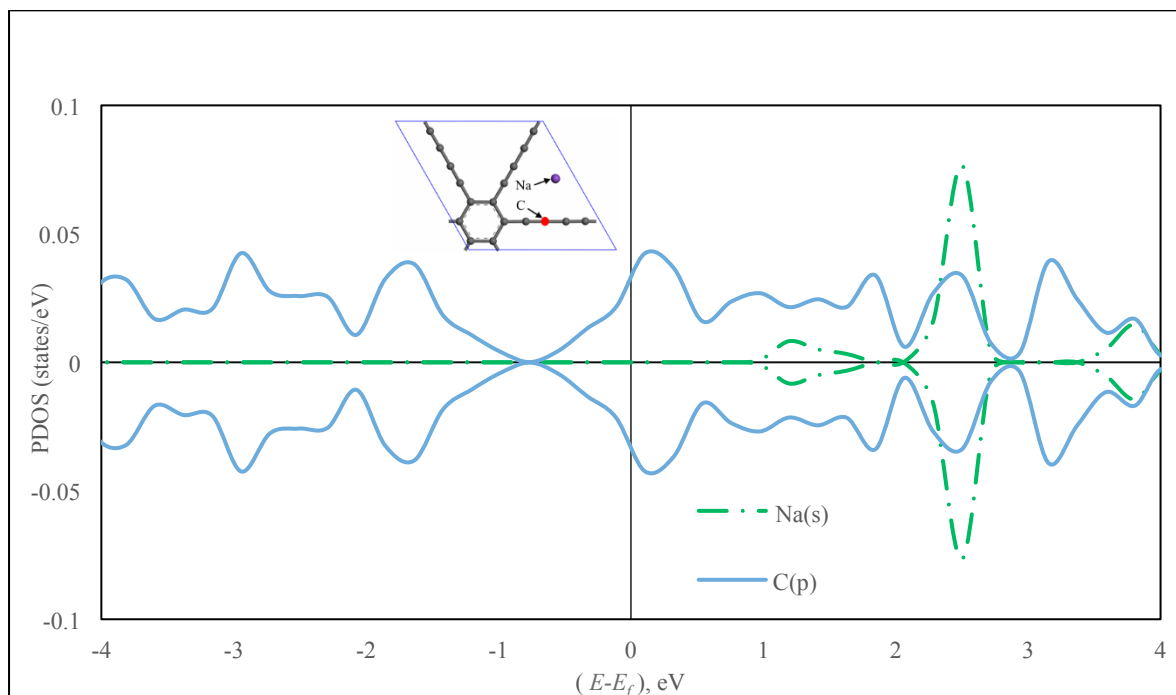


Figure S3. Na(s) (green dot-dashed line) and C(p) (blue solid line) partial densities of states for a system consisting of an Na atom on a single unit cell of GDY. The inset shows the structure of the system with the Na atom shown as a purple ball and the C atoms as grey balls. The C atom considered is highlighted in red (i.e. the second carbon atom of the 4-carbon chain of GDY). The energy shown is relative the Fermi energy, E_f .